American Mineralogist, Volume 74, pages 981–993, 1989

Two-phase nickeliferous monosulfide solid solution (mss) in megacrysts from Mount Shasta, California: A natural laboratory for nickel-copper sulfides

WILLIAM E. STONE, MICHAEL E. FLEET, NEIL D. MACRAE
Department of Geology, University of Western Ontario, London, Ontario N6A 5B7, Canada

ABSTRACT

Sulfide spherules in basalt and andesite tephra from a cinder cone on Mount Shasta, California, have been characterized in detail. The nickel-iron-copper sulfides occur in micrometer-sized subspherical polymineralic aggregates with an unidentified opaque hydrous iron silicate within olivine and pyroxene megacrysts, along fractures in the megacrysts, and in altered glass. The sulfide minerals include monosulfide solid solution (mss), pentlandite and chalcopyrite, and minor pyrrhotite, violarite, pyrite, idaite, and Fe-rich intermediate solid solution (iss). Mss is generally S-rich (>53 at.% S) and occurs as two largely intergrown lamellar phases: mss(1) with 6.2 to 12.0 at.% Ni and mss(2) with 13.9 to 19.7 at.% Ni. Pentlandite coexisting with mss or violarite is Ni-rich, whereas that coexisting with pyrrhotite is relatively Fe-rich and is invariably S-rich. The proportion of sulfide minerals present in an aggregate and within the volume of a handspecimen varies markedly, but sulfides in olivine megacrysts have relatively more mss(2) and relatively less chalcopyrite.

The phase relations for the iron-nickel sulfides bear only a fair correspondence to those of low-temperature laboratory studies. In particular, the observed miscibility gap in mss is on the Fe-rich side of the system, and the field of mss(2) does not extend to the Ni-rich side. The extent of unmixing of mss is variable even within a single bomb sample, but this may reflect annealing on a cooling gradient. The subspherical shape of the sulfide mineral aggregates and the consistency of bulk sulfide and olivine compositions with experimental high-temperature partitioning data suggest an origin through sulfide liquid immiscibility. However, the presence of many sulfide aggregates along fractures and in dacitic matrix and the variable bulk sulfide composition contradict an interpretation of sulfide liquid immiscibility and suggest instead that high-temperature subsolidus processes, such as degassing, S infiltration along fractures, and Ni diffusion, may have been important.

INTRODUCTION

Most nickel-copper sulfide ores consist of pentlandite, pyrrhotite, and chalcopyrite and may have exsolved at low temperature from high-temperature monosulfide solid solution (mss; e.g., Naldrett and Kullerud, 1967). Knowledge of the subsolidus phase relations and cooling history of mss is therefore necessary to understand fully the origin of nickel-iron-copper sulfide minerals and of nickel-copper sulfide ores. The subsolidus phase relations of mss are known from experimental study in the system Fe-Ni-S (Naldrett et al., 1967; Kullerud et al., 1969; Misra and Fleet, 1973; Craig, 1973) and are supported by study of the composition and phase relations of quenched single-phase mss with up to 17.1 at.% Ni in samples of basalt (Desborough et al., 1968; Skinner and Peck, 1969; Kanehira et al., 1973; Mathez, 1976; Czamanske and Moore, 1977) and nodules in kimberlite, lherzolite, or eclogite (Desborough and Czamanske, 1973; Frick, 1973; Bishop et al., 1975; de Waal and Calk, 1975; Haggerty, 1975; Meyer and Boctor, 1975; Peterson and Francis, 1977; Clarke, 1979; Haggerty et al., 1979; Tsai et al., 1979; Boctor and Boyd, 1980; Botkunov et al., 1980; Hunter and Taylor, 1984).

In this paper, mss occurring in samples of basalt and andesite tephra from a cinder cone on Mount Shasta, California (Anderson, 1974a, 1974b) with as much as 19.7 at.% Ni is described in detail, and its origin and phase relations are discussed and interpreted. The mss is unmixed (two-phase) in the form of a lamellar intergrowth and occurs with pentlandite, chalcopyrite, and an unidentified opaque hydrous iron silicate as micrometer-sized, subspherical aggregate inclusions within megacrysts of olivine, orthopyroxene, and clinopyroxene. The mss from Mount Shasta is the most Ni-rich reported in nature and, therefore, presents an opportunity for comparison with the phase relations determined experimentally for relatively Ni-rich bulk compositions in the Fe-Ni-S system.

0003–004X/89/0910–0981$02.00

TABLE 1. Composition of the megacrysts (wt%)

Sample:	5A	5M	5K	5K	5Y	5C	5C
Description:	ol	ol	ol core	ol margin	opx	cpx core	cpx margin
SiO_2	38.80	40.31	39.20	37.81	56.75	50.12	52.73
TiO_2	0	0.01	0	0.03	0.06	0.60	0.16
Al_2O_3	0.01	0.02	0.03	0.03	0.80	2.34	1.34
FeO	11.75	9.41	7.24	13.53	5.73	11.87	3.75
Cr_2O_3	0	0.13	0.02	0	0.61	0.25	0.66
MnO	0.13	0.13	0.10	0	0.11	0.19	0.08
MgO	48.99	49.8	53.12	48.36	33.31	14.36	19.83
CaO	0.15	0.15	0.12	0.14	1.66	18.67	20.28
Na_2O	0.01	0.03	0.01	0	0.07	0.58	0.31
NiO	0.18	0.23	0.24	0.15	0.06	0	0.05
Total	100.02	100.22	100.08	100.30	99.16	99.01	99.19
Fo (%)	88	90	93	86			
Wo (%)					3	39	40
En (%)					88	42	54
Fs (%)					9	19	6

Note: ol, olivine; opx, orthopyroxene; cpx, clinopyroxene.

PETROGRAPHY AND MINERAL CHEMISTRY

Experimental details

The Mount Shasta region of northern California is underlain by Pleistocene and Holocene lava and pyroclastic rocks of basaltic, andesitic, and dacitic composition (Anderson, 1974a). The samples for this study were obtained in 1977 from the Holocene cinder cone labeled S-17 (Anderson, 1974a), which is on the northern flank of Mount Shasta. The samples were in the form of bombs of dense olivine-phyric and olivine- and plagioclase-phyric basalt and basaltic andesite removed from a quarry face in the cinder cone. The section exposed has been divided into lower and upper strata (Anderson, 1974a). Sample 1 is from the east end of the lower strata, sample 5 is from 50 feet (about 15 m) west of a vent in the lower strata, and sample 6 is from the vent area. Samples 5A, 5B, 5C, 5K, 5L, 5M, 5N, 5X, 5Y, and 5Z are polished thin sections of sample 5. Several polished thin sections were prepared from about 10 bomb samples. The sulfide aggregates had a very limited distribution and, where more abundant, were present at less than 0.01 modal percent. More than half the thick sections did not contains sulfides, and only sample 5 yielded visible sulfides in most polished sections prepared from it.

Electron-microprobe analyses of the sulfide and silicate minerals were made with a JEOL JXA-8600 automated Superprobe, with synthetic NiS and FeS, natural chalcopyrite, and natural silicate minerals as standards. Analyses were made at 15 kV, 10 nA, 20 s or 20000 total counts, and a beam diameter of 2 μm. All analyzed sulfide areas were checked by EDS analysis. The counting time for Ni in megacryst phases was 50 s, and that for Ni, Cu, and S in glass was 100 s. The Ni content for glass was calibrated against that of a standard basalt glass (UWO2) with 169 ppm Ni (cf. Fleet et al., 1977, 1981). Repeated analyses of the standards used for analyses of the silicate minerals and the sulfide minerals indicate an accuracy relative to absolute element concentrations of within 0.5 wt% for SiO_2, FeO, MgO, and CaO; 0.04 wt% for NiO; and 1 wt% for Fe, Ni, Cu, and S.

Megacrysts

The olivine megacrysts are euhedral, rounded to irregular, single or composite grains that are generally unzoned and range in composition from Fo_{88} to Fo_{93} (Table 1), which is less magnesian than the analyses of Anderson (1974a; Fo_{94}). However, where the grain margin is intergrown with the matrix, as in sample 5K, it is relatively more Fe-rich (Fo_{86}).

The orthopyroxene megacrysts are unzoned spongy masses of composition $Wo_3En_{88}Fs_9$ (Table 1), which is more magnesian than the analysis of Anderson (1974a; $Wo_6En_{76}Fs_{18}$). The clinopyroxene megacrysts are large, optically zoned and twinned euhedra or composite grains, with or without orthopyroxene. Single clinopyroxene megacrysts have an Fe-rich core of $Wo_{39}En_{42}Fs_{19}$ composition (Table 1), which resembles the relatively Fe-rich clinopyroxene analysis of Anderson (1974a; $Wo_{39}En_{43}Fs_{18}$), in abrupt contact with a broad margin of $Wo_{39-40}En_{54-55}Fs_{6-7}$ composition, which is more magnesian than the more magnesian clinopyroxene analysis of Anderson (1974a; $Wo_{39}En_{50}Fs_{11}$). Locally, the clinopyroxene megacrysts are spongy at the grain margin.

Subspherical to irregular inclusions of the rock matrix occur within the megacrysts, particularly within the orthopyroxene megacrysts. They consist of dark reddish-brown glass, sulfide mineral aggregates, and microlites of plagioclase and clinopyroxene. The glass is rhyodacite with high Al_2O_3 and FeO/MgO ratio, low MgO (<2 wt%) and volatiles, and very low Ni, Cu, and S contents (Table 2). The glass analyses were made of spots 10 to 50 mm away from the included sulfide mineral aggregates, and the relatively high Ni content of the glass in sample 5Y may reflect contamination from the sulfides. The glass analyses have much higher SiO_2 contents than the analyses of glass (basalt to andesite) given in Table 2 of Anderson (1974a).

TABLE 2. Composition of the glass and the opaque iron silicate (wt%)

	Glass				Opaque iron silicate		
Sample:	5Y	5Y	5S	5S	5A	5K	5M
Glass in:	opx	mx	opx	mx			
SiO_2	66.87	70.53	70.15	69.04	19.62	15.40	18.87
TiO_2	1.34	1.58	1.34	1.41	0.11	0.10	0.12
Al_2O_3	13.00	11.99	14.19	13.16	0.12	0.13	0.04
FeO	8.93	7.48	5.84	7.47	68.30	70.32	68.94
Cr_2O_3	0	0.02	0.01	0	0.09	0.04	0.41
MnO	0.06	0.12	0.02	0.04	0.07	0.09	0.11
MgO	1.56	1.56	0.90	0.94	0.15	0.07	0.05
CaO	4.83	3.33	3.66	3.94	1.17	0.63	0.82
Na_2O	2.85	1.79	3.58	3.73	0	0.07	0
K_2O	2.85	2.00	0.70	0.97	0.16	0.11	0.03
Cu	0.01	0.00	0.00	0.00	n.d.	n.d.	n.d.
S	0.01	0.00	0.00	0.00	n.d.	n.d.	n.d.
Ni*	0.015	0.005	0.0052	0.0040	n.d.	n.d.	n.d.
NiO	n.d.	n.d.	n.d.	n.d.	0.24	0.44	0.33
Total	100.96	100.41	100.39	100.70	89.79	86.96	89.39

* Represents Ni content scaled to the Ni content of UWO2 glass.

An unidentified opaque hydrous iron silicate (Table 2) with optical properties similar to goethite and hereafter referred to as opaque iron silicate comprises as much as 40% of the subspherical shape of many sulfide mineral aggregates in thin section (Fig. 1). The opaque iron silicate also occurs as tiny irregular replacements along cracks and irregular bodies at the intersection of cracks in the megacrysts. It probably represents alteration of earlier iron sulfide and, to a lesser extent, silicate host.

Sulfide mineral aggregates

The sulfide minerals present include monosulfide solid solution (mss), pentlandite, and chalcopyrite and minor pyrrhotite, violarite, intermediate solid solution (iss), idaite, and pyrite. They occur generally with the opaque iron silicate mainly as 5- to 100-μm subspherical to irregular aggregate inclusions within the megacrysts and rarely as single, irregular-shaped grains in the rock matrix (Fig. 1). Locally, sulfide aggregates occur along fractures in megacrysts and appear to replace the megacryst parallel to the fracture trend. They occur also in glass-bearing inclusions, particularly within orthopyroxene. Although sulfide aggregates within the megacrysts commonly contain the assemblage mss, pentlandite, and chalcopyrite, sulfide aggregates with either two-phase mss or unmixed, nickeliferous mss are more common in olivine megacrysts, whereas chalcopyrite is more common in pyroxene megacrysts.

Many of the sulfide mineral aggregates consist of unmixed, two-phase mss with or without exsolved pentlandite (Figs. 1, 2), whereas other sulfide aggregates are composed of discrete grains of sulfide minerals. Violarite is spatially associated with pentlandite at the edge of an aggregate in sample 5Y, whereas pyrite occurs in aggregate form with mss and pentlandite in 5X, with violarite and chalcopyrite in 5B, and as a large isolated grain in the matrix of 5F. Chalcopyrite occurs as a discrete phase not always near the edge of an aggregate. Iron-rich intermediate solid solution (iss) is present in an isolated occurrence as a small grain in an altered, largely pyrrhotite-bearing aggregate within clinopyroxene, whereas idaite is present in an isolated occurrence as a very small grain aggregate with pentlandite within orthopyroxene.

The mss occurs as single-grain lamellar intergrowths (sample 5A, Fig. 2A). Individual lamellae are lathlike or flamelike, and their appearance in polished section clearly varies markedly with grain orientation. In Figure 2A, the lamellae are fine (1–3 μm thick) and homogeneously mixed, whereas in transverse section, they are coarser (5–20 μm) and appear to be heterogeneously mixed. The lamellae represent two unmixed $(Fe,Ni)_{1-x}S$ compositions. Electron-microprobe spot analysis and backscattered-electron images (Fig. 2B) confirm that the light phase of sample 5A in Figure 2A (which is the major or matrix phase) is relatively Ni-rich (15.3 at.% Ni) and the dark phase is Fe-rich (11.1 at.% Ni) (Fig. 3). We have labeled these two phases mss(2) and mss(1), respectively. They are not directly equivalent to the mss(2) and mss(1) of either Misra and Fleet (1973) or Craig (1973). As noted below, the mss(2) phase of Misra and Fleet (1973) is much more Ni-rich than the present mss(2), but the present mss(1) would logically represent a more evolved form of the Fe-rich solid solution [mss(1)] of Misra and Fleet (1973) and Craig (1973).

The mss grain of sample 5X (Fig. 4) was removed from a polished thick section and examined by X-ray precession photography (Fig. 5). Reflections of two intergrown and crystallographically aligned NiAs-type phases are present (cf. Fleet and MacRae, 1969). From the unit-cell parameters and d_{102} subcell spacing, these phases are identified as mss(1) and mss(2) (e.g., Naldrett et al., 1967; Misra, 1972): for mss(1), $a = 3.41$, $c = 5.62$, $d_{102} = 2.040$ Å, and for mss(2), $a = 3.41$, $c = 5.38$, $d_{102} = 1.983$ Å (relative to the NiAs-type subcell). The present d_{102} and compositional data (Table 3) for mss(1) and mss(2) are in approximate agreement with the data of Naldrett et al. (1967) for mss quenched from 600 °C. The stronger X-ray reflections are those of mss(2), indicating that it is the

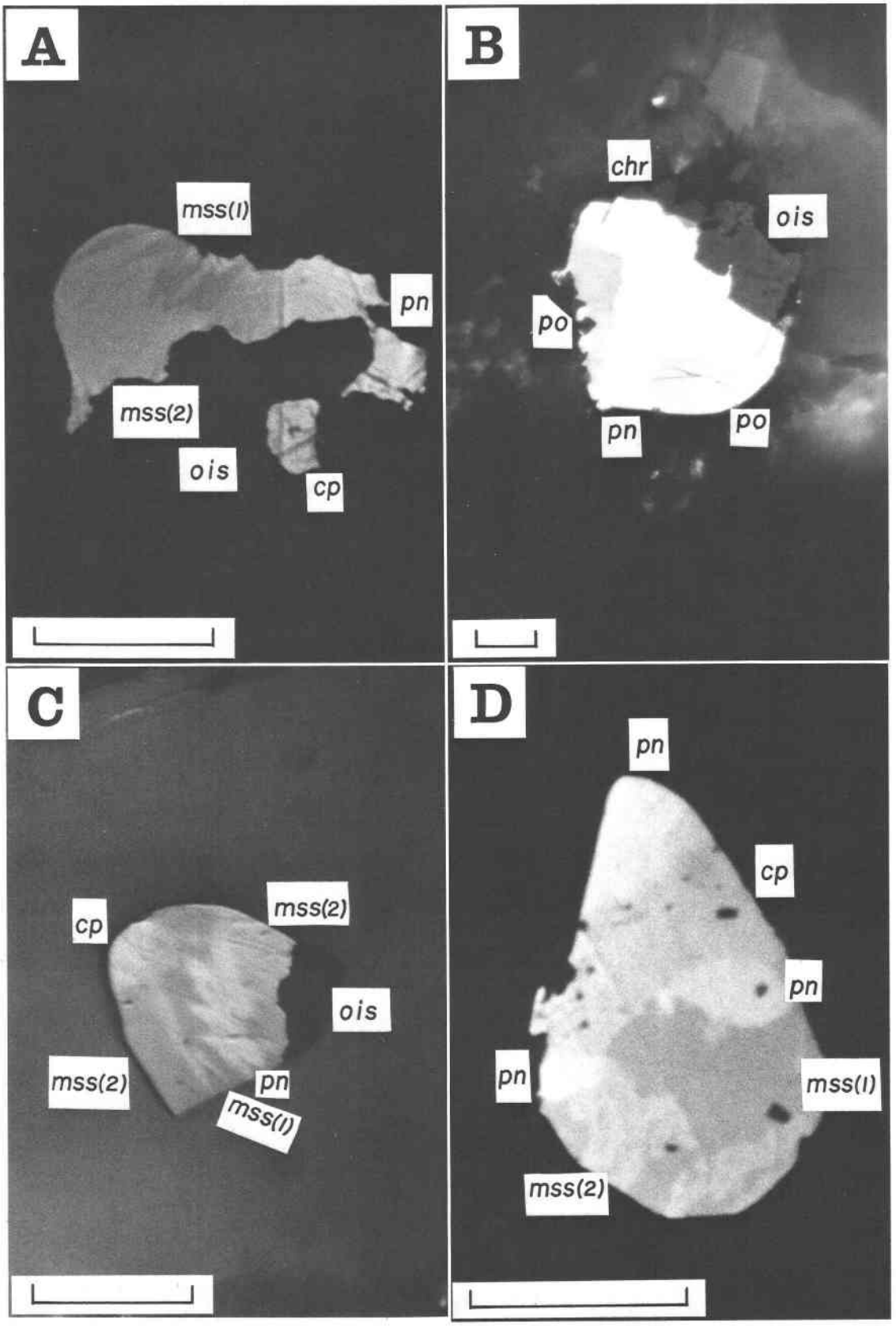
A
mss(1)
pn
mss(2)
ois
cp
B
chr
ois
po
pn
po
C
cp
mss(2)
ois
mss(2)
pn
mss(1)
D
pn
cp
pn
pn
mss(1)
mss(2)

major (or matrix) phase in the mss intergrowth, which is consistent with the relative proportions of mss(1) and mss(2) observed in the polished section of this sample. The precession photograph (Fig. 5) shows that apparently both mss(1) and mss(2) have the 3*C* superstructure (Fleet, 1968, 1971), which is consistent with their S-rich composition. Also present in the original photograph (but not reproduced in Fig. 5) are reflections of pentlandite, which exhibits the orientation relationship with mss of exsolved pentlandite in natural and synthetic nickeliferous pyrrhotite (Francis et al., 1976).

The compositional data for the sulfide phases given in Table 3 are an electron-microprobe spot analysis or averages of two to four electron-microprobe spot analyses for each phase. Computed standard deviations for the averaged composition of the sulfides are within 2.1 wt% for elements present in excess of 10 wt%, 1.3 wt% for elements present in the range of 5 to 10 wt%, 0.6 wt% for elements present in the range of 1 to 5 wt%, and 0.17 wt% for elements present in amounts less than 1 wt%. Microprobe analysis was complicated by the fine grain size and the (unavoidable) imperfectly polished surfaces. Analyses that were clearly contaminated by adjacent phases or that resulted in very low totals (less than 95 wt%) were not included in the averaged values. However, the small but anomalous contents of Ni in chalcopyrite and iss and of Cu in pyrrhotite, pentlandite, and iss and, to an unknown extent, the excess S over the nominal content of pentlandite reported in Table 3 may all represent secondary fluorescence interference. These compositional anomalies are less pronounced or absent in analyses of larger grains of other samples.

Most of the mss analyses have a cation total of 0.86–0.90 on the basis of one S, revealing that mss(1) and mss(2) are relatively S-rich (>53 at.% S; Table 3, Figs. 3, 4). The observed range in composition for mss(1) is 6.2 to 12.0 at.% Ni and for mss(2) is 13.9 to 19.7 at.% Ni. The compositional gap between the mss(1) and mss(2) in a particular sulfide mineral aggregate is variable, but is narrowest in sample 5A; the distinction of mss(1) and mss(2) here may be obscured by contamination from the adjacent lamellae during analysis. Although mss(2) occurs in the olivine-, orthopyroxene- and clinopyroxene-hosted aggregates, it is generally more common in the former, and it always coexists with mss(1). Mss(1), however, commonly occurs without mss(2), particularly in the clinopyroxene-hosted aggregates.

The one seemingly uncontaminated pyrrhotite analysis (sample 1) has a cation total of 0.93, 0.27 at.% Ni, and does not have detectable Cu (Table 3; Fig. 3). Alternatively, the pyrrhotite analyzed in samples 5M and 5E-1 is likely contaminated because the former has significant Ni (1.2 at.%) and coexists with pentlandite, whereas the latter has a low total and significant Ni (1 at.%) and coexists with pentlandite.

Analyses of the large and homogeneous pentlandite grains (samples 5K-3, 5L, 6-1, and 5E-1), where the likelihood of contamination from other phases is minimal, have a metal to S ratio of 1.097 to 1.116, 26.4 to 31.1 at.% Ni, and as much as 0.5 at.% Cu (Table 3, Figs. 3, 4). The metal to S ratio is less than the nominal 1.125, but it is within the range of pentlandite analyses made elsewhere (Harris and Nickel, 1972; Misra and Fleet, 1973). The most Ni-poor grains of pentlandite are those that coexist with pyrrhotite (samples 5M and 5E-1) rather than with mss or violarite. The composition of pentlandite within orthopyroxene and clinopyroxene generally resembles that of pentlandite within olivine.

The analyses of violarite indicate variable Ni and S contents and a metal to S ratio that exceeds the nominal 0.750 (Table 3, Fig. 3). Similar metal-rich violarite has been described elsewhere (Desborough and Czamanske, 1973). The pyrite grain in sample 5F seems devoid of Ni, whereas the pyrite in sample 5X has 0.58 at.% Ni and that in sample 5B has 1.33 at.% Ni (Table 3, Figs. 3, 4). However, the coexistence of the latter with violarite suggests that its relatively large Ni content may reflect contamination.

The analyses of relatively large grains indicate that chalcopyrite is nearly stoichiometric, with less than 0.50 at.% Ni (Table 3). The presence of approximately 21 wt% Cu and nearly twice as much Fe as Cu in the Cu-bearing mineral in sample 1 suggests it may be Fe-rich intermediate solid solution (iss) (Table 3, e.g., Barton, 1973; Cabri, 1973). However, the low weight percent total of the averaged analysis indicates contamination by adjacent opaque iron silicate. Similarly, the low total and significant Si content of the averaged analysis of idaite together with its small size suggests contamination from the adjacent orthopyroxene during analysis.

Sulfide phase relations

There is general agreement that mss is a complete solid solution between $Fe_{1-x}S$ and $Ni_{1-x}S$ to at least 400 °C, but below 400 °C, its phase relations are much debated (Naldrett and Kullerud, 1967; Naldrett et al., 1967; Misra

←

Fig. 1. (**A**) Olivine-hosted sulfide mineral aggregate 5C-4 in sample 5C. Mss(1) (dark gray), mss(2) (medium gray), pentlandite (pn, bright), chalcopyrite (cp, bright), and opaque iron silicate (ois, dark). (**B**) Olivine-hosted sulfide mineral aggregate in sample 5M. Pyrrhotite (po, medium gray), pentlandite (pn, bright), chromite (chr, dark gray), and opaque iron silicate (ois, dark). (**C**) Orthopyroxene-hosted sulfide mineral aggregate 5L. Mss(1) (dark gray), mss(2) (medium gray), chalcopyrite (cp, pale gray), pentlandite (pn, bright), and opaque iron silicate (ois, dark). (**D**) Clinopyroxene-hosted sulfide mineral aggregate inclusion 5C-1 in sample 5C. Mss(1) (darkest), mss(2) (medium gray), chalcopyrite (cp, medium gray) and pentlandite (pn, bright). Polished sections, reflected light, oil; scale bars represent 0.01 mm.

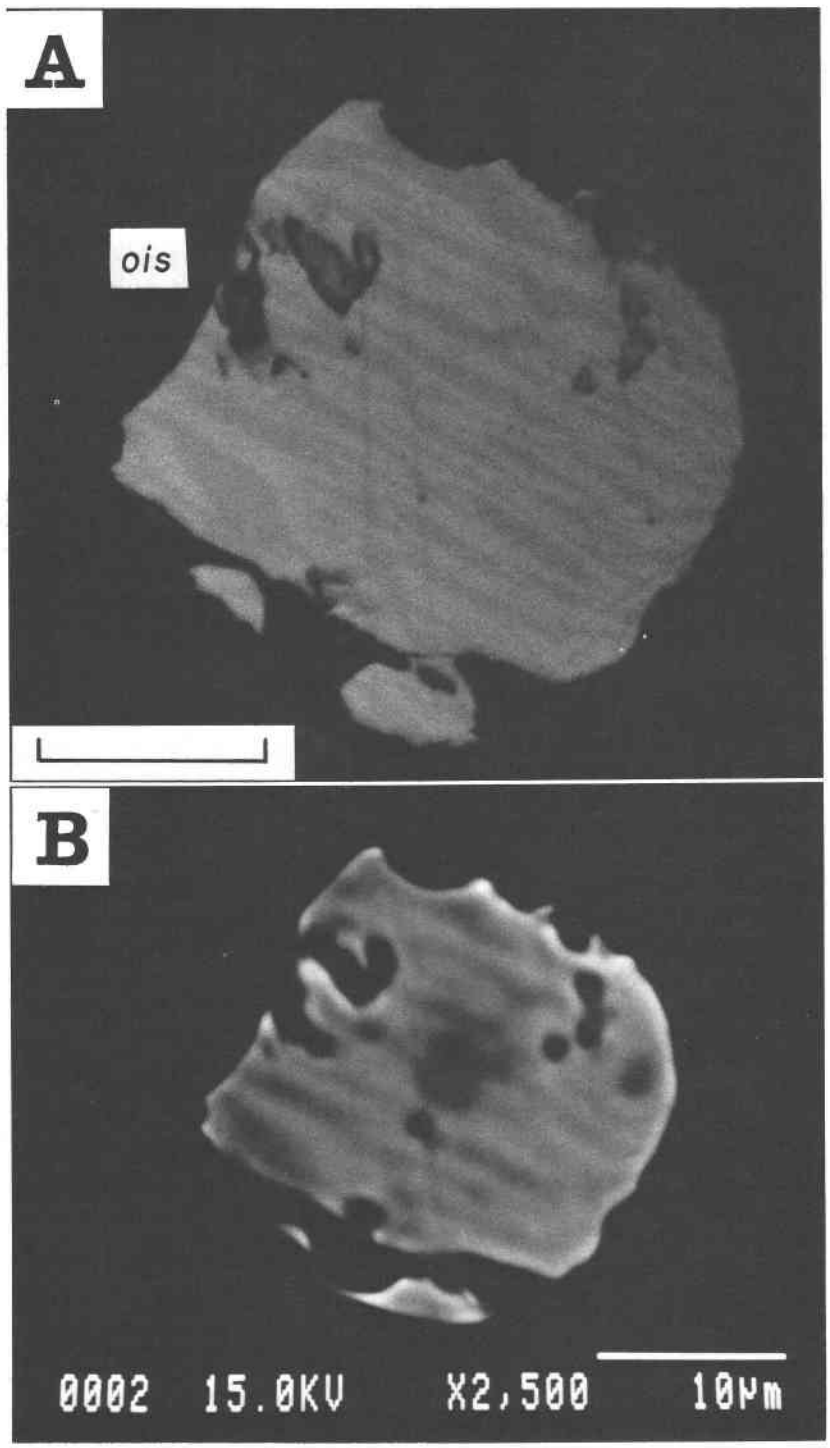

Fig. 2. (**A**) Two-phase lamellar intergrowth of mss(1) (dark) and mss(2) (light) in sample 5A with the opaque iron silicate (ois): polished section, oil; scale bar represents 0.01 mm. (**B**) Backscattered-electron image of the same area as (A); mss(1) is dark and mss(2) is light.

and Fleet, 1973; Craig, 1973; Barker, 1983). According to Misra and Fleet (1973), the continuity of the mss phase field between $Fe_{1-x}S$ and $Ni_{1-x}S$ breaks down between 400 and 300 °C, at a composition of about 33 at.% Ni. This result was in agreement with Shewman and Clark (1970), who reported a miscibility gap at a similar composition but at a slightly lower temperature (275 ± 10 °C). At 300 °C, Misra and Fleet (1973) observed that the

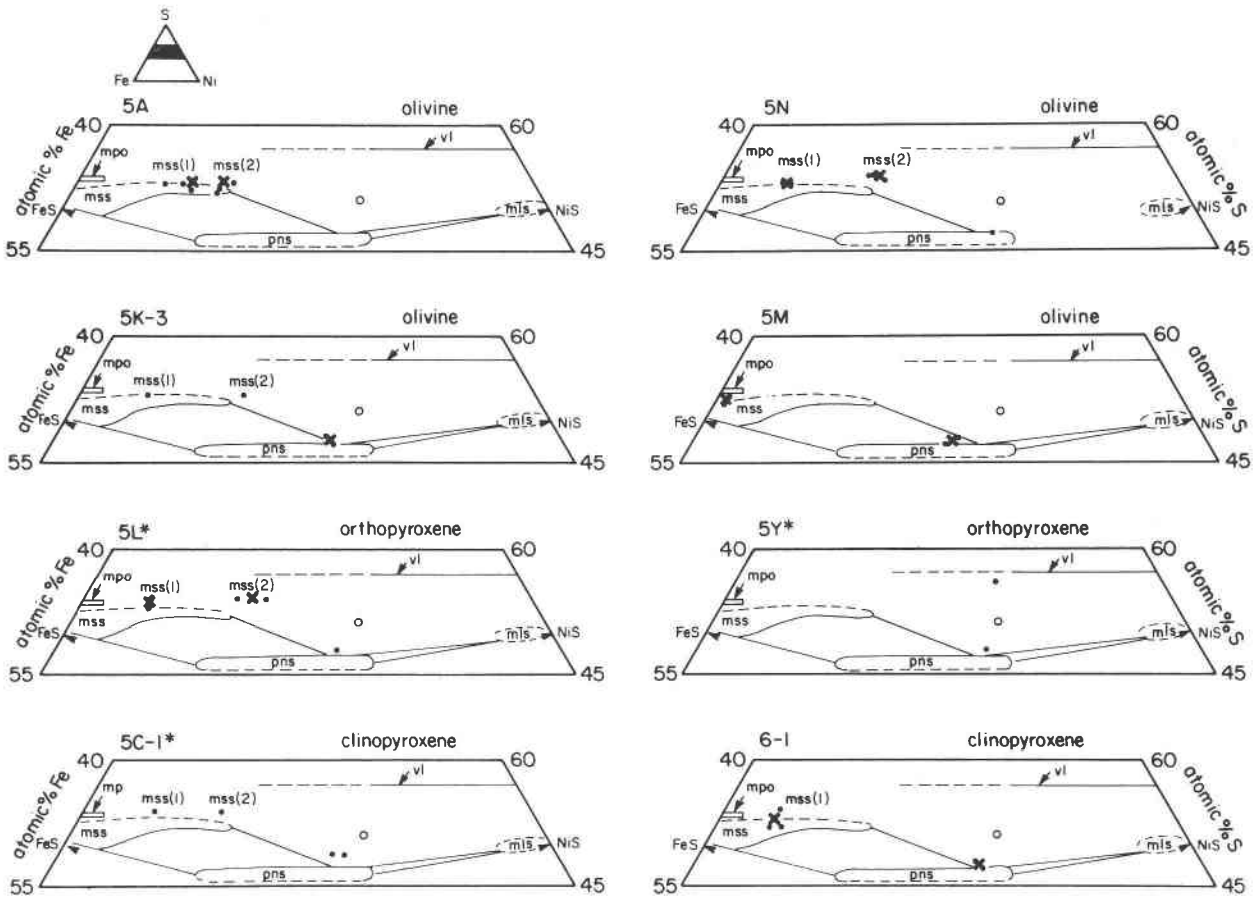

Fig. 3. Composition of sulfide phases within the Fe-Ni-S system. Dots are representative analyses, X represents averaged values of Table 3, and * denotes chalcopyrite-bearing sulfide mineral assemblages. Experimental phase relations for 230 °C from Misra and Fleet (1973) are for reference purposes only: megacryst host indicated top right. O is the composition of mss(2) from Misra and Fleet (1973).

mss field withdraws away from the Ni-S join and separates into two mss phases, mss(1) and mss(2), with about 25 and 33 at.% Ni, respectively, which coexist with pentlandite solid solution (about 33.5 at.% Ni). At lower temperatures, the mss(1) phase field withdraws further toward the Fe-S join, to about 17 at.% Ni at 230 °C, whereas mss(2) fails to change much from its composition at 300 °C. Pyrite-pentlandite tie-lines are first established at about 280 °C, whereas monoclinic pyrrhotite and pentlandite coexist only when the mss(1) field has withdrawn to at least 10 at.% Ni.

In contrast to Misra and Fleet (1973), Craig (1973) found that mss is a complete solid solution between $Fe_{1-x}S$ and $Ni_{1-x}S$ until 282 °C, where millerite crystallizes. At 263 ± 13 °C, a miscibility gap appears in mss at 18.5 at.% Ni, below which two phases coexist, mss(1) and mss(2). A miscibility gap forms in mss(2) at 225 ± 12 °C, near 26.3 at.% Ni, which Craig (1973) has suggested may correspond to the gap reported by Misra and Fleet (1973) at 300 °C. Below 250 °C, the miscibility gap expands such that between 225 and 200 °C, pentlandite and pyrite coexist. Final decomposition of the mss phases occurs below 100–200 °C.

For all the sulfide mineral aggregates from the Mount Shasta cinder cone, the miscibility gap between mss(1) and mss(2) is in the interval 12.0 and 15.3 at.% Ni (15.5 to 18.9 wt%), and largely within the mss(1) phase field of Misra and Fleet (1973) and Craig (1973) (Figs. 3, 4). The actual extent of miscibility varies from sample to sample; 7 to 17.4 at.% Ni in sample 5X and 11.1 to 15.3 at.% Ni in sample 5A. Coincidentally, this natural miscibility gap resembles more closely that between nickeliferous pyrrhotite solid solution and nickeliferous mss found in samples of medium tenor nickel sulfide ore heated under laboratory conditions to 500 and 540 °C (McQueen, 1979). However, previous experimentation under more controlled conditions (Misra and Fleet, 1973; Craig, 1973) failed to detect any evidence of a miscibility gap in mss at 500–540 °C within the Fe-Ni-S system.

Compared to previous experimental studies, the miscibility gap is in the more Fe-rich part of the Fe-Ni-S system. The large mss(2) phase field postulated by Craig

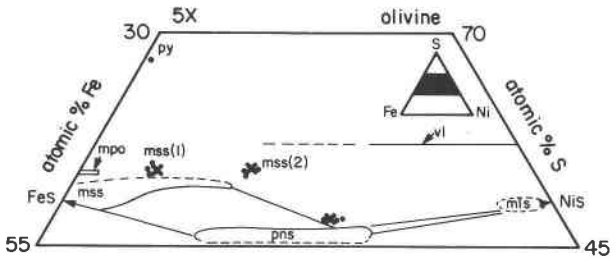

Fig. 4. Composition of phases in sulfide mineral aggregates of sample 5X used for precession photograph of Fig. 5 (see Fig. 3).

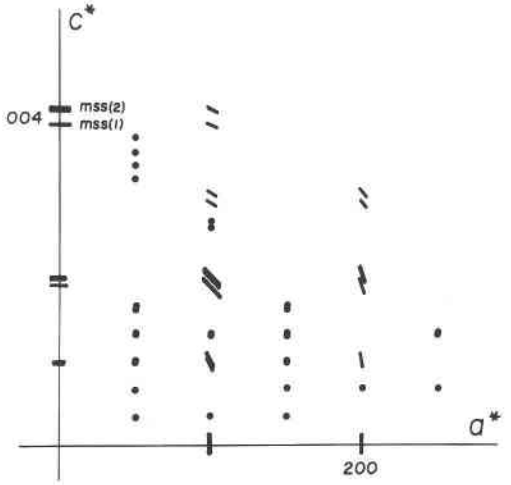

Fig. 5. Representation of part of zero-level X-ray precession film of sulfide aggregate 5X (Fig. 4; Table 3). NiAs-type subcell reflections are streaked due to mosaic spread. $3C$ superstructure reflections are represented by small dots. Mo$K\alpha$, $\bar{\mu} = 20°$, 3 d.

(1973) to extend across the Ni-rich side of the Fe-Ni-S system appears to be absent. It is replaced by pyrite-pentlandite, pyrite-pentlandite-violarite, and pentlandite-violarite assemblages (Figs. 3, 4), which is consistent with laboratory experimentation (Misra and Fleet, 1973). The discrepancies between the Mount Shasta and laboratory phase relations may reflect different bulk compositions, the presence of additional components, such as Cu, and disequilibrium in both the laboratory experiments and in nature at low temperatures (<300 °C).

We recognize that the products of laboratory annealing experiments would be reaction-path dependent at these low temperatures and that the Mount Shasta sulfides might represent reheated material previously equilibrated to near-surface temperatures. However, the phase relations shown by the Mount Shasta cinder cone would represent extension of the Misra and Fleet (1973, 1974) phase relations to lower temperatures. The present miscibility gap might then be a second, lower-temperature unmixing event. The persistence of the restricted and somewhat stranded mss(2) composition of Misra and Fleet (1973) is certainly a curious feature, but the present mss(2) field appears to behave in a similar manner. The present mss-pentlandite tie-lines are generally consistent with those of Misra and Fleet (1973), whereas the present S-rich mss compositions are comparatively inconsistent. By extrapolation of the progressive withdrawal of the mss(1) solvus of Misra and Fleet (1973) to more Fe-rich compositions with reduction in temperature, the average mss compositions at Mount Shasta unmixed between 180 and 220 °C, the mss(1) of samples 5K-3, 5L, 5C-1, 5N, and 5X (Figs. 3, 4) equilibrated at about 140 °C, and the sulfide mineral aggregates with pyrrhotite equilibrated at about 90 °C.

Although the pentlandite in the Mount Shasta sulfide aggregates tends to contain more Cu than coexisting mss or pyrrhotite, its Cu content and that of mss does not appear to increase with increased Fe content (e.g., Hill, 1983), and the S contents of relatively Ni-rich and Ni-poor pentlandite are similar. Pyrite in nickel-copper sulfide assemblages has generally been considered to be of secondary origin (Bishop et al. 1975; MacLean, 1977), although cooling of mss from high temperature should result in exsolution of pyrite and vaesite with or without violarite from compositions along the S-rich boundary of mss (Naldrett and Kullerud, 1967; Naldrett et al., 1967). Pyrite in the Mount Shasta samples coexists with mss in sample 5X, but does appear to be secondary in samples 5F and 5B. Craig (1973) has attributed the difficulty he had in nucleating pyrite during formation of pyrite-pentlandite assemblages along the S-rich boundary of mss to the short time for experimentation compared to that in nature. By analogy, the lack of pyrite exsolution in the samples from Mount Shasta, and in sulfide mineral aggregates from other localities, may reflect relatively rapid cooling. Consequently, the mss remains relatively S-rich metastably.

Although stable to 461 °C, violarite, like pyrite, is difficult to nucleate in experimental studies (Craig, 1973), and its presence in nature is generally attributed to alteration of pentlandite (Craig and Scott, 1974; Misra and Fleet, 1974). The spatial association of violarite with pentlandite and the opaque iron silicate in the Mount Shasta samples is consistent with its formation by alteration of pentlandite. The opaque iron silicate most likely formed by low-temperature hydrothermal alteration of the Mount Shasta cinder cone, perhaps contemporaneously with the formation of secondary pyrite and violarite.

Petrogenesis

Sulfide mineral aggregates similar to but less Ni-rich than those from the cinder cone at Mount Shasta have been reported in megacrysts within samples of nodules from kimberlite (Haggerty, 1975; Clarke, 1979; Haggerty et al., 1979; Boctor and Boyd, 1980; Botkunov et al., 1980; Hunter and Taylor, 1984), nodules from lherzolite and eclogite xenoliths (Bishop et al., 1975; Tsai et al., 1979), and in samples of basalt (Skinner and Peck, 1969;

TABLE 3. Composition of minerals in the sulfide mineral aggregates

Sample	Phase	Host	Fe	Ni	Cu	S	Fe	Ni	Cu	S
			(at.%)				(wt%)			
5A	mss(1)	ol	36.17	11.09	0	52.74	45.60	14.69	0	38.14
5A	mss(2)	ol	32.11	15.28	0	52.61	40.55	20.29	0	38.16
5M	pn	ol	26.09	26.41	0.04	47.47	31.83	33.69	0.05	33.26
5M	po	ol	46.44	1.18	0	52.38	58.87	1.57	0	38.12
5K-1	mss(1)	ol	39.35	7.00	0	53.65	50.92	9.52	0	39.87
5K-1	mss(2)	ol	29.13	19.68	0.02	51.13	36.37	25.90	0.02	36.65
5K-3	mss(1)	ol	40.45	6.70	0.01	52.84	51.70	9	0.02	38.77
5K-3	mss(2)	ol	29.68	16.87	0.03	53.42	37.61	22.47	0.04	38.86
5K-3	pn	ol	23.53	28.66	0.13	47.69	29.16	37.34	0.19	33.94
5N	pn	ol	21.98	30.75	0	47.26	27.00	39.71	0	33.33
5N	mss(1)	ol	39.82	7.02	0	53.17	51.54	9.55	0	39.51
5N	mss(2)	ol	30.11	16.12	0	53.77	38.61	21.73	0	39.51
5X	mss(1)	ol	39.09	7.02	0	53.90	49.70	9.38	0	39.35
5X	mss(2)	ol	28.77	17.37	0.01	53.84	36.46	23.14	0.03	39.17
5X	pn	ol	23.10	28.51	0.03	48.36	27.82	36.10	0.04	33.45
5X	py	ol	32.00	0.58	0	67.41	44.24	0.85	0	53.50
5C-4	mss(1)	ol	32.99	11.98	0.02	54.99	41.16	15.74	0.02	39.21
5C-4	mss(2)*	ol	26.95	18.31	0.02	54.72	34.75	24.81	0.03	40.31
5C-4	cp	ol	24.64	1.17	23.17	51.02	28.80	1.45	30.94	34.08
5C-4	pn	ol	21.29	31.13	0.18	48.40	25.24	37.65	0.24	32.30
5B	vl*	ol	6.22	40.80	0.16	52.82	7.77	53.64	0.16	37.66
5B	cp*	ol	24.70	0	24.47	50.82	30.03	0	34.00	35.30
5B	py*	ol	31.20	1.38	0	67.41	44.71	2.07	0	55.17
5Y	cp	gls	24.13	0.10	24.39	51.38	29.08	0.12	33.60	35.40
5Y	pn	gls	20.92	30.52	0.19	48.37	24.95	38.35	0.26	32.97
5Y	vl	gls	18.46	25.99	0.18	55.37	23.16	34.34	0.27	39.68
5L	cp	opx	25.55	0.14	23.48	50.84	30.75	0.17	32.16	35.14
5L	pn	opx	22.62	29.23	0.48	47.67	27.69	37.62	0.67	33.51
5L	mss(1)	opx	38.91	7.21	0	53.90	49.82	9.70	0	39.66
5L	mss(2)	opx	28.59	17.42	0.03	53.97	36.64	23.45	0.04	39.71
5Z	id*	opx	11.46	0.89	39.60	48.05	12.86	1.05	50.76	30.81
5Z	pn*	opx	22.54	28.79	0.35	48.32	27.33	36.79	0.49	33.49
5C-1	mss(1)*	cpx	38.79	7.25	0.01	53.95	50.36	9.91	0.02	40.02
5C-1	mss(2)*	cpx	31.72	13.86	0.04	54.38	41.02	18.88	0.06	41.02
5C-1	cp*	cpx	24.27	0.30	23.79	51.64	29.67	0.38	33.23	36.06
5C-1	pn	cpx	21.85	28.60	0.83	48.72	25.89	35.70	1.13	32.99
6-1	mss(1)	cpx	40.93	6.39	0.02	52.66	51.97	8.54	0.04	38.34
6-1	pn	cpx	22.83	29.46	0.42	47.30	27.11	36.72	0.57	32.70
1	po	cpx	49.79	0.27	0	51.95	61.33	0.37	0	38.26
1	iss	cpx	32.64	0.15	15.06	52.16	39.98	0.19	20.99	36.68
5F	py	mx	32.80	0	0	67.20	47.36	0	0	54.92
5E-1	po	cpx	45.34	0.97	0.02	53.47	56.90	1.28	0.02	38.33
5E-1	pn	cpx	25.48	26.38	0.13	47.93	30.51	33.23	0.18	32.89
5E-4	mss(1)	cpx	40.44	6.20	0	53.37	50.41	8.13	0	38.20
5E-4	pn*	cpx	21.59	29.85	0.22	48.33	25.20	36.66	0.29	34.43
5E-4	cp	cpx	25.05	0.06	24.00	50.89	28.90	0.07	31.51	33.70

Note: mss(1) is relatively Ni-poor mss, mss(2) is relatively Ni-rich mss, pn is pentlandite, po is pyrrhotite, vl is violarite, cp is chalcopyrite, py is pyrite, iss is intermediate solid solution, id is idaite, ol is olivine, opx is orthopyroxene, cpx is clinopyroxene, and gls is glass.

* Analyses with as much as or more than 0.50 at.% Si.

Czamanske and Moore, 1977). These sulfide mineral aggregates have analogous mineral assemblages and equivalent host-rock associations to ore deposits of nickel-copper sulfides and may have been formed by similar processes. Therefore, the petrogenesis of sulfide mineral aggregates is of some importance because of the potential for insight into both the S content of upper-mantle peridotites and the origin of nickel-copper ore deposits. The models commonly invoked for the genesis of nickel-copper sulfides range from the formation of an immiscible sulfide liquid during the early magmatic stage of the host rocks, either by segregation (e.g., Naldrett, 1981) or assimilation (e.g., Lesher and Groves, 1986), to sulfide metasomatism during the late-magmatic stage or subsolidus history under conditions that excluded chemical equilibration between the silicate minerals (e.g., olivine) and the sulfides (e.g., Fleet, 1979; Fleet and MacRae, 1983).

Features invoked by proponents of sulfide liquid immiscibility include the association with mafic and ultramafic rocks, a bulk sulfide composition within the boundaries of mss in the system Cu-Fe-Ni-S (Boctor and Boyd, 1980), and the subspherical shape of sulfide mineral aggregates. The subspherical shape of a sulfide mineral aggregate, in particular, is generally considered to indicate that it was a sulfide droplet that remained liquid as the host solidified, following segregation of the sulfide liquid from the parental silicate melt and inclusion within either cumulate silicate minerals or in the matrix (Skinner and Peck, 1969; Czamanske and Moore, 1977).

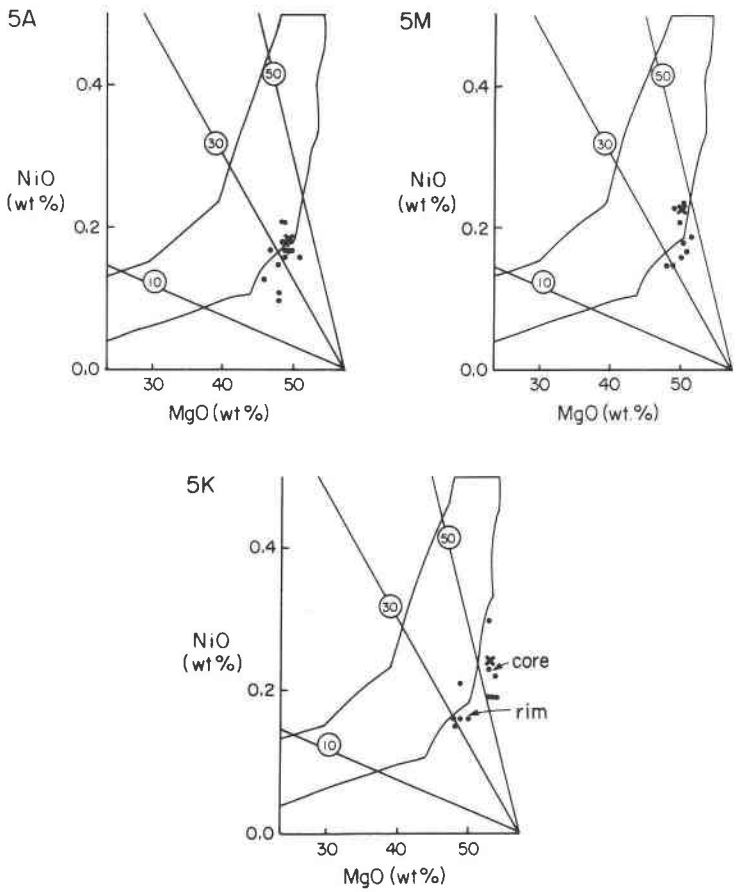

Fig. 6. Plot of NiO vs. MgO contents of olivine megacryst hosts and Ni partitioning data (K_{D3} = 33; Fleet et al., 1977; Fleet and MacRae, 1983, 1988). Dots are individual spot analyses; X represents averaged values given in Table 1. The lines that originate from the lower right corner are isopleths of constant NiS content.

Crystallization of a sulfide liquid droplet is considered generally to follow the crystallization and subsolidus changes determined by experimental study in the systems Fe-Ni-Cu-S (Craig and Kullerud, 1969; Hill, 1983) and Fe-Ni-S and Fe-Cu-S (Naldrett et al., 1967; Kullerud et al., 1969; Misra and Fleet, 1973; Craig, 1973; Craig and Scott, 1974). Cooling to approximately 1100 °C fosters crystallization of mss, consuming nearly all the Ni in the droplet, and the residual sulfide liquid is Cu-rich. Progressive cooling below 610 °C forces exsolution of pentlandite from the mss, which eventually converts to pyrrhotite. Cu within the mss is partitioned into pentlandite or exsolves as chalcopyrite. Sulfide mineral aggregates with mss preserved and intricate intergrowth textures are considered to be quenched.

The residual, Cu-rich liquid separates from the mss at 850 °C (Craig and Kullerud, 1969) and crystallizes as iss. At approximately 550 °C, the iss recrystallizes to chalcopyrite and Fe-rich iss (Barton, 1973; Cabri, 1973; Boctor and Boyd, 1980; Haggerty et al., 1979), which with low-temperature re-equilibration, recrystallizes to chalcopyrite and pyrrhotite (MacLean, 1977). Ni in iss exsolves as pentlandite.

Fleet et al. (1977), Fleet (1979), and Fleet and MacRae (1983) noted that the composition of olivine associated with nickel-copper sulfides is incompatible with equilibration under magmatic conditions. For nickel-copper sulfide deposits that have not been metamorphosed beyond low-grade conditions, the NiO contents of olivine are too high, and, correspondingly, the NiS contents of the sulfides are too low, relative to laboratory partition data. Metamorphosed deposits exhibit a progressive approach to equilibrium values with increase in metamorphic grade (Fleet and MacRae, 1983). Recent experimentation (Fleet and MacRae, 1987, 1988) has investigated the exchange of Ni/Fe between olivine and monosulfide-oxide liquid at 1300–1395 °C under controlled atmosphere conditions. The distribution coefficient (K_{D3}) is essentially constant at about 30 to 35 in the temperature range 900 to 1400 °C for olivine of composition Fo_{97} to Fo_0, monosulfide composition with up to 70 mol% NiS, and a wide range of f_{O_2} and f_{S_2}. K_{D3} exhibits only a weak decrease from 35 to 29 with increase in f_{O_2} from the iron-wüstite (IW) buffer to close to the fayalite-magnetite-silica phase (FMQ) buffer. In comparison, calculated K_{D3} values for komatiite-hosted nickel-copper sulfides range

from 2 to 5. The olivines in these komatiites have far too much NiO to have been equilibrated with the nickel-copper sulfides in the early magmatic stage. Alternatively, equilibration of olivine and sulfide compositions might not be expected if the sulfides had been formed by metasomatic replacement during either the late magmatic stage or in the subsolidus history. One other feature of nickel-copper sulfides inconsistent with the early magmatic (immiscible sulfide liquid) models is the erratic variation in bulk sulfide composition, between orebodies, within orebodies, and within individual handspecimens (Fleet, 1978, 1979). There is no correlation of bulk sulfide composition with magmatic fractionation index. The marked variation in the composition of the nickel-copper sulfide blebs in handspecimen samples of disseminated ore from the Frood mine, Sudbury, Ontario is clearly inconsistent with an origin through sulfide liquid immiscibility (Fleet, 1978).

Features of the sulfide mineral aggregates from Mount Shasta, such as their subspherical shape and bulk compositions, which plot in the mss field of the system Fe-Ni-S, appear consistent with formation by liquid immiscibility. Furthermore, the NiO contents of many of the olivine megacrysts are more-or-less consistent with high-temperature equilibration with the included sulfide mineral aggregates (Fig. 6). A sulfide aggregate from the same cinder cone as the present study, when homogenized by heating, gave a bulk sulfide composition of 40 mol% NiS, 49.3 at.% S (Anderson, 1974b). This is consistent with estimates of the maximum NiS content of the present olivine megacryst–hosted sulfides, which is probably greater than the average mss composition (26–30 mol% NiS) and less than the coexisting pentlandite composition (Figs. 3, 4).

Thus the sulfide aggregates may have been original inclusions in the megacryst crystals: segregated sulfide blebs trapped during crystal growth either from the parental picritic melt (Anderson, 1974a) or in a peridotitic source region (the megacrysts being xenocrysts). One problem with this reconstruction is the large variability in the chemical composition and mineral assemblage of the Mount Shasta sulfide aggregates. Variable Ni/Cu ratio in nickel sulfide ores and sulfide mineral aggregates has been attributed to fractionation of immiscible sulfide liquid (Craig and Kullerud, 1969; Czamanske and Moore, 1977; MacLean, 1977). Accordingly, the relatively greater Ni/Cu ratio of the olivine-hosted aggregates could reflect the presence, during olivine crystallization, of a Ni-rich sulfide liquid that fractionated to a more Cu-rich liquid as the coexisting silicate liquid crystallized fractionated orthopyroxene and clinopyroxene. However, if the olivine, orthopyroxene, and clinopyroxene megacrysts were comagmatic and coeval, this would not be a very satisfactory explanation. Anderson (1974a) suggested that only olivine and orthopyroxene fractionated until the olivine composition reached 16 wt% FeO, whereupon clinopyroxene fractionated. Extrapolation to the composition of the liquids that coexisted with the megacrysts by using distribution coefficients for equilibrium low-pressure olivine-liquid partitioning of TiO_2 (0.02), orthopyroxene-liquid partitioning of TiO_2 (0.1), and clinopyroxene-liquid partitioning of TiO_2 (0.3) (Pearce and Norry, 1979; Grove and Bryan, 1983) and by using equilibrium low-pressure olivine-liquid partitioning of FeO/MgO (0.3), orthopyroxene-liquid partitioning of FeO/MgO (0.27), and clinopyroxene-liquid partitioning of FeO/MgO (0.29) (Roeder and Emslie, 1970; Green et al., 1979; Stolper, 1980) suggests that the olivine, orthopyroxene, and magnesian clinopyroxene coexisted with magma of similar FeO/MgO and TiO_2 contents and are comagmatic and indeed megacrysts, whereas the Fe-rich clinopyroxene cores coexisted with liquid higher in FeO/MgO and TiO_2. These results reflect the mixing of picritic and andesitic magma during petrogenesis of the Mount Shasta rocks (Anderson, 1974a), a process more characteristic of high-level crustal magmatism than magmatism in the mantle.

As a second magmatic explanation, the basaltic and andesitic magmas may have become S-saturated through assimilation immediately before eruption (e.g., Lesher and Groves, 1986). Infiltration of sulfide liquid along fractures in the megacrysts could then have resulted in formation of the sulfides and equilibration. Alternatively, a late-stage S-enriched fluid phase might be a more effective metasomatizing agent.

Several features of the sulfide mineral aggregates from Mount Shasta, such as the presence of nickeliferous aggregates in dacitic glass-bearing inclusions within the megacrysts, alignment of many aggregates along cracks in the magacrysts, and wide variation in bulk sulfide composition (e.g., Ni/Fe and Ni/Cu ratios, Figs. 3, 4) are consistent with formation by subsolidus processes. We note, in passing, that the subspherical shape of many of the sulfide aggregates should not be regarded as unambiguous evidence for a precursor sulfide liquid droplet because it could be a manifestation of high-temperature subsolidus replacement processes (below). Also bulk sulfide composition within the Fe-Ni-Cu system is defined by whole-rock composition. High-temperature rock-fluid processes would certainly result in bulk sulfide composition identical to that expected from sulfide liquid immiscibility.

The megacryst-bearing basalt and andesite tephra could have been sulfidized by hot gases during formation of the cinder cone. Isolated pyrite grains in the matrix indicate that S-bearing fluids were present later in the cooling history of the volcanic rocks (prior to the cinder cone activity) by degassing during or following eruption. In this process, S saturation results from quenching of the erupted lava, and S-rich gas is expelled from the quenched glass (Moore and Fabbi, 1971). Condensation of the S-rich gas in fractures and vesicles forms sulfide liquid droplets that interact with accumulated silicate minerals at high temperature. Ni and Fe scavenged from olivine react with the sulfide to form mss. Degassing has been considered for the formation of some sulfide mineral aggregates, globules, and spherules in samples of MORB (Moore and

Calk, 1971; Frick, 1973; Mathez and Yeats, 1976; MacLean, 1977). The presence of nickeliferous sulfides within dacitic glass inclusions in the margins of the orthopyroxene megacrysts certainly indicates mobility of chalcophile metals during the subsolidus history of these rocks. Independent evidence of the mobility of chalcophile metals under high-temperature subsolidus conditions comes from the presence of small amounts of Ni, Fe, and Cu in sublimate over some lavas of Hawaii (Naughton et al., 1974). Whether the sulfide mineral aggregates from Mount Shasta formed by sulfide liquid immiscibility or subsolidus processes is as yet unresolved. However, the possibility of their formation in response to degassing deserves further consideration.

The foregoing discussion emphasizes the ambiguous nature of the petrographic and geochemical features usually associated with sulfide liquid immiscibility. The association of nickel-copper sulfides with mafic and ultramafic rocks, a bulk sulfide composition within the boundaries of mss, intricate intergrowth textures, and subspherical shape do not collectively constitute unique evidence of quenched immiscible sulfide droplets. They are equally consistent with formation of the sulfides by *high-temperature* subsolidus processes. As long as equilibrium is attained (or approached), the bulk sulfide composition is still defined by ambient f_{O_2}, f_{S_2}, temperature, and bulk compositions.

Acknowledgments

We thank R. L. Barnett and D. M. Kingston for their assistance with the electron-microprobe analysis and John Forth for the preparation of thin sections. Critical comments by S. D. Scott and an anonymous reviewer were very helpful. The research was funded by a Natural Sciences and Engineering Research Council of Canada operating grant to M.E.F.

References cited

Anderson, A.T. (1974a) Evidence for a picritic, volatile-rich magma beneath Mount Shasta, California. Journal of Petrology, 15, 243–267.

——— (1974b) Chlorine, sulfur, and water in magmas and oceans. Geological Society of America Bulletin, 85, 1483–1492.

Barker, W.W. (1983) The Fe-Ni-S system + (Co,Cu), CSIRO Report no. FP 26, 81 p.

Barton, P.B. (1973) Solid solution in the system Cu-Fe-S. Part 1. The Cu-S and Cu-Fe-S joins. Economic Geology, 68, 433–465.

Bishop, F.C., Smith, J.V., and Dawson, J.B. (1975) Pentlandite-magnetite intergrowth in De Beers spinel lherzolite. Review of sulphides in nodules. Physics and Chemistry of the Earth, 9, 323–328.

Boctor, N.Z., and Boyd, F.R. (1980) Ilmenite nodules and associated sulphides in kimberlite from Yakutia, U.S.S.R. Carnegie Institution of Washington Year Book, 1979, 302–304.

Botkunov, A.I., Goranin, V.K., Kudryavtseva, G.P., and Perminova, A. (1980) Mineral inclusions in olivine and zircon from the kimberlite pipe "Mir." Doklady Akademii Nauk SSSR, 251, 1233–1236.

Cabri, L.J. (1973) New data on phase relations in the Cu-Fe-S system. Economic Geology, 68, 443–454.

Clarke, D.B. (1979) Synthesis of nickeloan djerfisherites and the origin of potassic sulphides at the Frank Smith Mine. In F.R. Boyd and H.O.A. Meyer, Eds., Proceedings of the second international kimberlite conference. The mantle sample: Inclusions in kimberlites and other volcanics, vol. 2, p. 300–308. American Geophysical Union, Washington, D.C.

Craig, J.R. (1973) Pyrite-pentlandite assemblages and other low temperature relations in the Fe-Ni-S system. American Journal of Science, 273A, 496–510.

Craig, J.R., and Kullerud, G. (1969) Phase relations in the Cu-Fe-Ni-S system and their application to magmatic ore deposits. Economic Geology, Monograph 4, 344–358.

Craig, J.R., and Scott, S.D. (1974) Sulfide phase equilibria. In P.H. Ribbe, Ed., Sulfide mineralogy. Mineralogical Society of America Reviews in Mineralogy, 1, CS-1–CS-110.

Czamanske, G.K., and Moore, J.G. (1977) Composition and phase chemistry of sulfide globules in basalt from the Mid-Atlantic Ridge rift valley near 37°N lat. Geological Society of America Bulletin, 88, 587–599.

Desborough, G.A., and Czamanske, G.K. (1973) Sulfides in eclogite nodules from a kimberlite pipe, South Africa, with comments on violarite stability. American Mineralogist, 58, 195–202.

Desborough, G.A., Anderson, A.T., and Wright, T.L. (1968) Mineralogy of sulfides from certain Hawaiian basalts. Economic Geology, 63, 636–644.

de Waal, S.A., and Calk, L.C. (1975) The sulfides in the garnet pyroxenite xenoliths from Salt Lake Crater, Oahu. Journal of Petrology, 16, 134–153.

Fleet, M.E. (1968) The superstructures of two synthetic pyrrhotites. Canadian Journal of Earth Sciences, 5, 1183–1185.

——— (1971) The crystal structure of a pyrrhotite (Fe_7S_8). Acta Crystallographica, 27, 1864–1867.

——— (1978) Origin of disseminated copper-nickel sulfide ore at Frood, Sudbury, Ontario. Economic Geology, 72, 1449–1456.

——— (1979) Partitioning of Fe, Co, Ni, and Cu between sulfide liquid and basaltic melts and the composition of Ni-Cu sulfide deposits—A discussion. Economic Geology, 74, 1517–1519.

Fleet, M.E., and MacRae, N.D. (1969) Two-phase hexagonal pyrrhotites. Canadian Mineralogist, 9, 699–705.

——— (1983) Partition of Ni between olivine and sulfide and its application to Ni-Cu sulfide deposits. Contributions to Mineralogy and Petrology, 83, 75–81.

——— (1987) Partition of Ni between olivine and sulfide: The effect of temperature, f_{O_2} and f_{S_2}. Contributions to Mineralogy and Petrology, 95, 336–342.

——— (1988) Partition of Ni between olivine and sulfide: Equilibria with sulfide-oxide liquids. Contributions to Mineralogy and Petrology, 100, 462–469.

Fleet, M.E., MacRae, N.D., and Hertzberg, C.T. (1977) Partition of nickel between olivine and sulfide: A test for immiscible sulfide liquid. Contributions to Mineralogy and Petrology, 32, 191–197.

Fleet, M.E., MacRae, N.D., and Osborne, M.D. (1981) The partition of nickel between olivine, magma and immiscible sulfide liquid. Chemical Geology, 32, 119–127.

Francis, C.A., Fleet, M.E., Misra, K., and Craig, J.R.. (1976) Orientation of exsolved pentlandite in natural and synthetic nickeliferous pyrrhotite. American Mineralogist, 61, 913–920.

Frick, C. (1973) The sulfides in griquaite and garnet-peridotite xenoliths in kimberlite. Contributions to Mineralogy and Petrology, 39, 1–16.

Green, D.H., Hibberson, W.O., and Jaques, A.L. (1979) Petrogenesis of mid-ocean ridge basalts. In M.W. McElhinny, Ed., The Earth: Its origin, structure and evolution, p. 265–269. Academic Press, London.

Grove, T.L., and Bryan, W.B. (1983) Fractionation of pyroxene-phyric MORB at low pressure: An experimental study. Contributions to Mineralogy and Petrology, 84, 293–309.

Haggerty, S.E. (1975) The chemistry and genesis of opaque minerals in kimberlites. Physics and Chemistry of the Earth, 9, 295–307.

Haggerty, S.E., Hardie, R.B., and McMahon, R.M. (1979) The mineral chemistry of ilmenite nodule associations from the Monastery diatreme. In F.R. Boyd and H.O.A. Meyer, Eds., Proceedings of the second international kimberlite conference, vol. 2, p. 249–256. The mantle sample: Inclusions in kimberlites and other volcanics. American Geophysical Union, Washington, D.C.

Harris, D.C., and Nickel, E.H. (1972) Pentlandite compositions and associations in some natural minerals. Canadian Mineralogist, 11, 861–878.

Hill, R.E.T. (1983) Experimental study of phase relations at 600° in a portion of the Fe-Ni-Cu-S system and its application to natural sul-

phide assemblages. In D.L. Buchanan and M.J. Jones, Eds., Sulphide deposits in mafic and ultramafic rocks, p. 14–21. The Institution of Mining and Metallurgy, London.

Hunter, R.H., and Taylor, L.A. (1984) Magma-mixing in the low velocity zone: Kimberlite megacrysts from Fayette County, Pennsylvania. American Mineralogist, 66, 16–29.

Kanehira, K., Yui, S., Sakai, H., and Sasaki, A. (1973) Sulfide globules and sulfur isotope ratios in abyssal tholeiite from the Mid-Atlantic Ridge near 30°N latitude. Geochemical Journal, 7, 89–96.

Kullerud, G., Yund, R.A., and Moh, G.H. (1969) Phase relations in the Cu-Fe-S, Cu-Ni-S, and Fe-Ni-S system. Economic Geology, Monograph 4, 323–343.

Lesher, C.M., and Groves, D.I. (1986) Controls on formation of komatiite-associated nickel-copper sulfide deposits. In G. Friedrich et al., Eds., Geology and metallogeny of copper deposits, p. 43–62. Springer-Verlag, Heidelberg.

MacLean, W.H. (1977) Sulfides in Leg 37 drill core from the Mid-Atlantic Ridge. Canadian Journal of Earth Sciences, 14, 674–683.

Mathez, E.A. (1976) Sulfur solubility and magmatic sulfides in submarine basalt glass. Journal of Geophysical Research, 81, 4269–4275.

Mathez, E.A., and Yeats, R.S. (1976) Magmatic sulfides in basalt glass from DSDP hole 319A and site 320, Nazca plate. In R.S. Hart et al., Eds., Initial reports of the Deep Sea Drilling Project, vol. 14, p. 363–373. U.S. Government Printing Office, Washington, D.C.

McQueen, K.G. (1979) Experimental heating and diffusion effects in Fe-Ni sulfide ore from Redross, Western Australia. Economic Geology, 74, 140–148.

Meyer, H.O.A., and Boctor, N.Z. (1975) Sulfide-oxide minerals in eclogite from Stockdale kimberlite, Kansas. Contributions to Mineralogy and Petrology, 52, 57–68.

Misra, K.C. (1972) Phase relations in the Fe-Ni-S system. Ph.D. thesis, London, Ontario, University of Western Ontario, 213 p.

Misra, K.C., and Fleet, M.E. (1973) The chemical compositions of synthetic and natural pentlandite assemblages. Economic Geology, 68, 518–539.

——— (1974) Chemical composition and stability of violarite. Economic Geology, 69, 391–403.

Moore, J.G., and Calk, L. (1971) Sulfide spherules in vesicles of dredged pillow basalt. American Mineralogist, 56, 476–488.

Moore, J.G., and Fabbi, B.P. (1971) An estimate of juvenile sulfur content of basalt. Contributions to Mineralogy and Petrology, 33, 118–127.

Naldrett, A.J. (1981) Nickel sulfide deposits: Classification, composition, and genesis. Economic Geology, 75th Anniversary Volume, 628–685.

Naldrett, A.J., and Kullerud, G. (1967) A study of the Strathcona mine and its bearing on the origin of the nickel-copper ores of the Sudbury district, Ontario. Journal of Petrology, 8, 453–531.

Naldrett, A.J., Craig, J., and Kullerud, G. (1967) The central portion of the Fe-Ni-S system and its bearing on pentlandite exsolution in iron-nickel sulfide ores. Economic Geology, 62, 826–847.

Naughton, J.J., Lewis, V.A., Hammond, D., and Nishimoto, D. (1974) The chemistry of sublimates collected directly from lava fountains at Kilauea Volcano, Hawaii. Geochimica et Cosmochimica Acta, 38, 1674–1690.

Pearce, J.A., and Norry, M.J. (1979) Petrogenic implications of Ti, Zr, Y, and Nb variations in volcanic rocks. Contributions to Mineralogy and Petrology, 69, 33–47.

Peterson, R., and Francis, D. (1977) The origin of sulfide inclusions in pyroxene megacrysts. American Mineralogist, 62, 1049–1051.

Roeder, P.L., and Emslie, R.F. (1970) Olivine-liquid equilibrium. Contributions to Mineralogy and Petrology, 29, 275–289.

Shewman, R.W., and Clark, L.A. (1970) Pentlandite phase relations in the Fe-Ni-S system and notes on the monosulfide solid solution. Canadian Journal of Earth Sciences, 7, 67–85.

Skinner, B.J., and Peck, D.L. (1969) An immiscible sulfide melt from Hawaii. Economic Geology, Monograph 4, 310–322.

Stolper, E.M. (1980) A phase diagram for mid-ocean ridge basalts: Implications for petrogenesis. Contributions to Mineralogy and Petrology, 74, 13–27.

Tsai, H., Shieh, Y., and Meyer, H.O.A. (1979) Mineralogy and S^{34}/S^{32} ratios of sulfides associated with kimberlite, xenoliths and diamonds. In F.R. Boyd and H.O.A. Meyer, Eds., Proceedings of the second international kimberlite conference. The mantle sample: Inclusions in kimberlites and other volcanics, vol. 2, p. 87–103. American Geophysical Union, Washington, D.C.

Manuscript received December 5, 1988
Manuscript accepted May 8, 1989